Journal of New Materials for Electrochemical Systems 14, 259-264 (2011)

Microstructure Analysis and Hydrolysis Mechanism of AlLi Alloys Activated by Metal Additives for Hydrogen Generation

Mei-Qiang Fan, Shu Liu, Wen-Qiang Sun, Da Chen, Chun-Ju Lv and Kang-ying Shu*

Department of Materials Science and Engineering, China JiLiang University, Hangzhou 310018, P.R. China

Received: May 30, 2011, Accepted: June 06, 2011, Available online: July 06, 2011

Abstract: *Microstructure analysis and hydrolytic mechanism of activated Al-Li alloys including low melting point metal additives X (X: indicated as Bi, Sn, In and Ga) are explained for their good hydrogen generation performance in this paper. It is demonstrated that the presence of these metals has a double effect. The metals are helpful to reduce the grain size of Al-Li alloys due to the formation of new intermetallic compounds such as $BiLi_3$, Sn_5Li_{13}, $AlLiIn_2$, etc., preventing the connection of Al-Al and Li-Li atoms. The metals strongly improved hydrogen generation performance because the metals deposited on the surface of Al and Li metals act as cathodic centers for hydrogen generation. There were dual micro galvantic cells between Al (Li) and metal additives created in the hydrolysis process which stimulated the electrochemical corrosion of Al and Li. The LiX alloy acts as the initial hydrolysis centers due to its low standard potential and its hydrolysis byproduct LiOH further accelerates the micro galvantic cell between Al and X. Therefore, hydrogen generation performance is linked to standard potential of metal additives, increased Li and X amounts, uniform distribution of Li and X in the Al matrix in the longer milling time. Our results show that the potential good hydrogen generation performance can be obtained via the design and preparation technology of Al alloys.*

Keywords: Hydrogen generation, nanocomposite, deformation and fracture, metals and alloys

1. INTRODUCTION

It is widely recognized that hydrogen is one of the most promising energy carriers as a clean alternative to fossil fuels for the future [1]. The low polluting emissions and high calorific value of hydrogen combustion make it a very attractive fuel in both mobile and stationary power generation [2, 3]. But the widespread use of hydrogen is severely hampered by the lack of safe and efficient hydrogen storage methods. The extensive studies of various hydrogen storage methods still can not be applied due to their shortcomings such as high cost, no safe, high decomposition, etc.. And there are no viable system that can reversibly store exceeding 5 wt.% hydrogen under mild conditions that is an indispensable requisite to fulfill the practical operation of proton exchange membrane fuel cell (PEMFC)[4]. In the current situation, on-demand hydrogen generation appears to provide a more realistic solution for near-term hydrogen storage applications.

Among many hydrogen generation materials, aluminum and its alloys are recognized to be one of the most suitable metal applicable for future hydrogen production, considered from cost, hydrogen generation density, etc.. There is a trend to utilize aluminum as an effective, user-friendly, and safe approach for hydrogen production in recent years [5, 6]. Aluminum and aluminum alloy have good stability near-neutral pH conditions due to dense passive film of oxides and hydrated oxides preventing (or slowing down) access of water to the metal surface [7]. In the study of the Al/H_2O system, the formation of a coherent and adherent oxide layer on the Al surface should be eliminated to maintain the sustainable reaction. Many reaction-promoting approaches are introduced and it has been demonstrated that additions of hydroxides, metal oxides or selected salts can effecitively disrupt the passivation layer [8-10]. In addition, alloying Al with low melting point metals has good ability to prevent the formation of a coherent passivation layer and increase Al reactivity [11-13]. Kravchenko found that Al-Ga alloy had 100% hydrogen yield at 333 K and its hydrolysis rate could be enhanced by In and Zn additives [14]. The milled Al-Bi alloy had good hydrolysis perfornamce at 298 K and approxi-

*To whom correspondence should be addressed: Email: shukangying@163.com

mate 1000 mL hydrogen/1 g Al alloy with 100% efficiency could be generated [15]. The improved Al reactivity was explained from that the low melting point metals ruined the passivation layer on the surface of aluminum metal and made the standard potential of aluminum shift negatively. However, these metals can not react with water to produce hydrogen and more addition of them will lead to lower hydrogen density. It was found that Al-Li alloy had high hydrogen generation amount and fast hydrolysis rate. Li can react with water to produce hydrogen and an alkali solution that can stimulate Al hydrolysis in water.

In the present study, we employ the milled Al-Li-X (X: Bi, Sn, In, Ga) alloy as the hydrogen generation materials and analyze its hydrolysis performance. The improved hydrogen generation performance is explained via microstructure analysis and hydrolysis mechanism. The aim of the work is expected to supply an effective method for design and preparation technology of Al alloys.

2. EXPERIMENTAL

2.1. Materials

Aluminum powder (99.9% purity, ~10 μm particle size; Beijing Xingry Technology Company, Ltd., China), Li flakes (99.9% purity; China Energy Lithium Co., Ltd., China), pure other metals (Beijing Xingry Technology Company, Ltd China) were used as starting materials. All reagents were used as received. The reagents were weighed and placed in 50 mL stainless steel jars to which stainless steel balls were added. The jars were kept in an argon-filled glove box. The ball-to-mixture weight ratio was 26 to 1. Milling for 15 h was done in a QM-3SPO$_4$ planetary ball miller at 450 r/min and a 0.2 MPa argon atmosphere, unless otherwise indicated.

2.2. Measurement of hydrogen evolution

The hydrolysis was carried out by adding Al−Li−X alloy (0.3 g) to water (100 mL) at 298 K and 1 atm. The alloy was pressed into a pellet in a stainless steel mold (10 mm diameter) under 5-ton pressure before addition. The released hydrogen gas flowed through a condenser and its volume was measured by water displacement in an inverted cylinder. The reaction time was calculated, taking the release of the first bubble as the start of the hydrolysis. The final volume of the hydrogen was collected within 1 h of the reaction.

2.3. Microstructure analysis

Powder X-ray diffraction (XRD) patterns of the prepared samples were obtained on an X-ray diffractometer (Thermo ARL X'TRA Switzerland,). Scanning electron microscopy (SEM) observations were performed using a JSM-5610LV (JEOL Co.) equipped with an INCA energy-dispersive X-ray spectrometer. The solid byproduct of hydrolysis was filtered using a vacuum pump, and then dried in an oven at 323 K for 24 h before measurements. Transmission electron microscopy (TEM) observations were performed using a JEM-2100 (JEOL Comp.) equipped with a selected area electron diffractometer. The support film had a pore size of 200 mesh. The measured samples were ultrasonically dispersed in anhydrous solvent for 1 h.

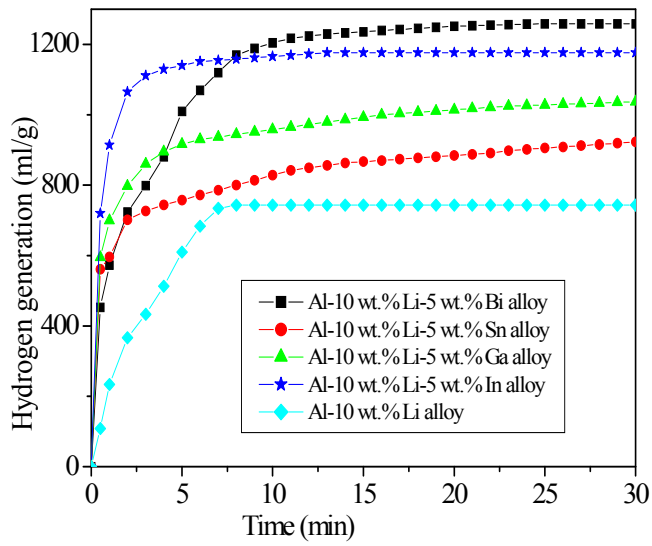

Figure 1. Hydrogen generation performance of Al-10 wt.% Li alloys with different metal additives.

3. RESULTS AND DISCUSSION

3.1. Al reactivity

Table. 1 and Fig. 1 show hydrogen generation performance of Al-Li-X (X: Bi, Sn, In, Ga) alloys in water. Al-10 wt.%Li alloy only yields 743 ml hydrogen/g with 53% efficiency, but with 5 wt.% other metal additives, the alloys have higher hydrogen generation performance, especially that the Al-10 wt.% Li-5 wt.%Bi alloy yields 1258 ml hydrogen/g with 95% efficiency. The Al-10 wt.%-5 wt% X alloys yield approximate 180-510 ml hydrogen/g higher than that of Al-10 wt.%Li alloy. Meanwhile, maximum hydrogen generation rate is also increased with the addition of X metals. Their value is increased from 108 ml /min.g to 594, 452, 719 and 561 ml /min.g with the addition of Bi, Sn, In, and Ga, respectively. The hydrogen generation process can be devided in to

Table 1. Hydrogen generation performance of Al-10 wt.% Li alloys with different metal additives

Alloys	Amount of generated hydrogen within 60 min (ml/g)	Maximum hydrogen genration rate (ml /min.g)	Total conversion %
Al-10wt.%Li	743	108	53
Al-10wt.%Li-5 wt.% Bi	1258	594	95
Al-10wt.%Li-5 wt.% Sn	930	452	70
Al-10wt.%Li-5 wt.% In	1036	719	78
Al-10wt.%Li-5 wt.% Ga	1176	561	88

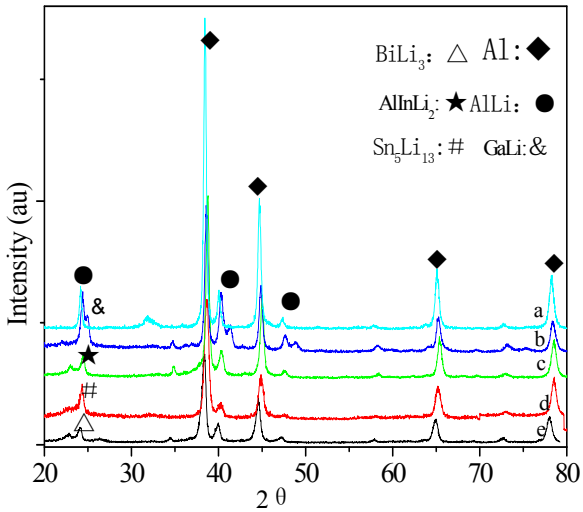

Figure 2. XRD patterns of different milled Al alloys. a, Al-10 wt%Li alloy; b, Al-10 wt% Li-5%Ga alloy; c, Al-10 wt% Li-5%In alloy; d, Al-10 wt% Li-5%Sn alloy; e, Al-10 wt% Li-5%Bi alloy.

two periods: high-hydrogen-generation-rate and low -hydrogen-generation-rate from the inflection point and most of hydrogen was generated in the first stage [16]. In Fig. 1, the second stage may not be observed due to the quick ending of hydrolysis reaction in the hydrolysis of Al-10 wt%Li alloy. It has been elaborated that Li hydrolysis quickly yeilded byproduct LiOH and LiOH stimulated Al hydrolysis before the formation of insoluble $LiAl_2(OH)_7$. But with the addition of other metals, there existed low-hydrogen-generation-rate after the quick hydrolysis reaction in the first stage. Obviously, the additives (Bi, Sn, In, Ga) changed the hydrolysis process of Al-10 wt.%Li alloy in some degrees.

3.2. Microstructure analysis of Al-Li-X(X: Bi, Sn, In ,Ga.)

Fig.2 shows the X−ray patterns of milled Al−10 wt%Li−5 wt%X (X: Bi, Sn, In, etc.) alloys. It is clear that peaks of new intermetallic compounds such as $BiLi_3$, Sn_5Li_{13}, $AlLiIn_2$, etc, are identified except the other phase compositions including Al, AlLi. The results reflect that the formation of the compounds proceeded in the milling process and LiX has lower formation enthalpy. Seith found that the enthalpy of formation of $BiLi_3$ from the pure solids was -77 kJ/mol from direct reaction calorimetry[17], lower than -41.763 kJ/mol of AlLi alloy [18]. With the addition of metal additives, the lines become broadened, reflecting the decrease of grain size, due to the formation of intermetallic compounds being formed in the milling process and preventing the connection of Al-Al and Li-Li. Peak broadening can be also attributed to changes in the lattice of Al due to repeated grain breakup, cold welding and re-welding. Continuous deformation of the Al lattice in the milling process is an important reason for an increased concentration of defects, dislocations as well as microstrains in the particles. Czech [10] have found that the increased concentration of defects and induced strains accelerated the electrochemical corrosion of Al in water. The Li/X molar has also a great effect on the formation of intermet-

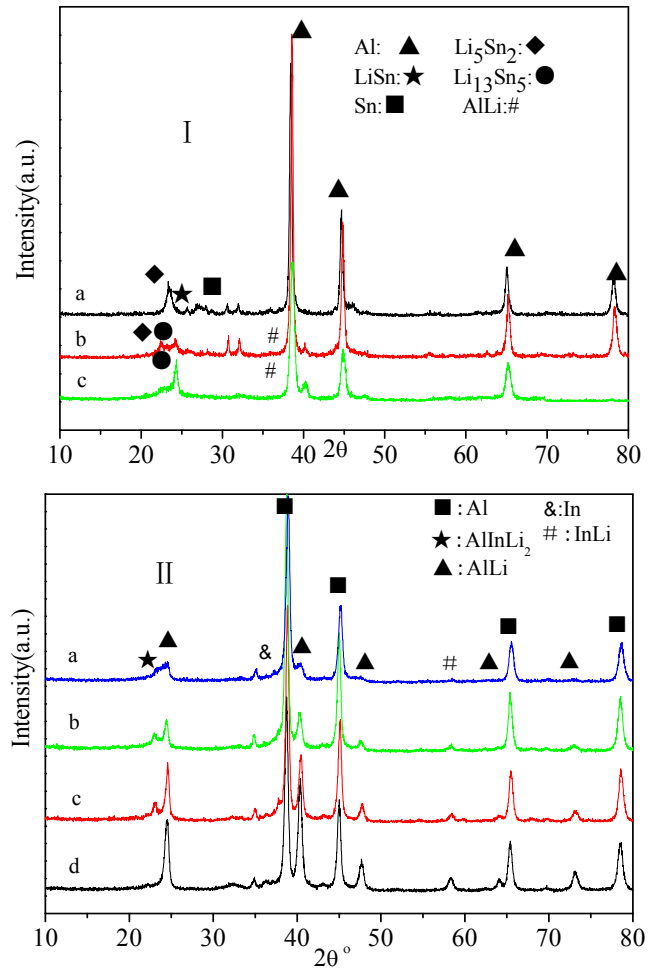

Figure 3. XRD patterns of different milled Al-Li-X alloys with different Li/X weight ratios. Ⅰ, Al alloy with different Li/Sn weight ratios. a, 1:7; b, 1:3; c, 1:1. Ⅱ, Al alloy with different Li/In weight ratios. a, 1:3; b, 1:1; c, 2:1; d, 3:1.

allic compounds. There is an evolution from simple to complex compound with the increase in Li/X molar ratio, which can be confirmed from Fig. 3. The phase evolution from LiSn and Li_5Sn_2 to $Li_{13}Sn_5$ is obtained with increasing Li/Sn weight ratio increasing from 1:7 to 1:1. The peaks of Sn, LiSn and Li_5Sn_2 can be clearly identified in the XRD patterns of aluminum alloys including Li/Sn weight ratio of 1:7. But these peaks disappear and only peaks of $Li_{13}Sn_5$ are found in the XRD patterns of aluminum alloy with Li/Sn weight ratio of 1:1. The same phenomenon can be also found in aluminum alloy including increased Li/In weight ratio.

Generally, the milled Al alloys has fairly small grain size, some particle size even ranges in hundreds of nm. Fig. 4 shows TEM of milled Al-Li-In alloy before and after hydrolysis. Some irregular particles are observed and crack surfaces maintain a non-rearranges and atomically rough structure. A lot of nano-/micro-cracks and defects could be generated in the milling process and they were partly responsible for the improved hydrolytic performance of milled Al-10 wt% Li alloy while the unmilled mixture of Al and Li

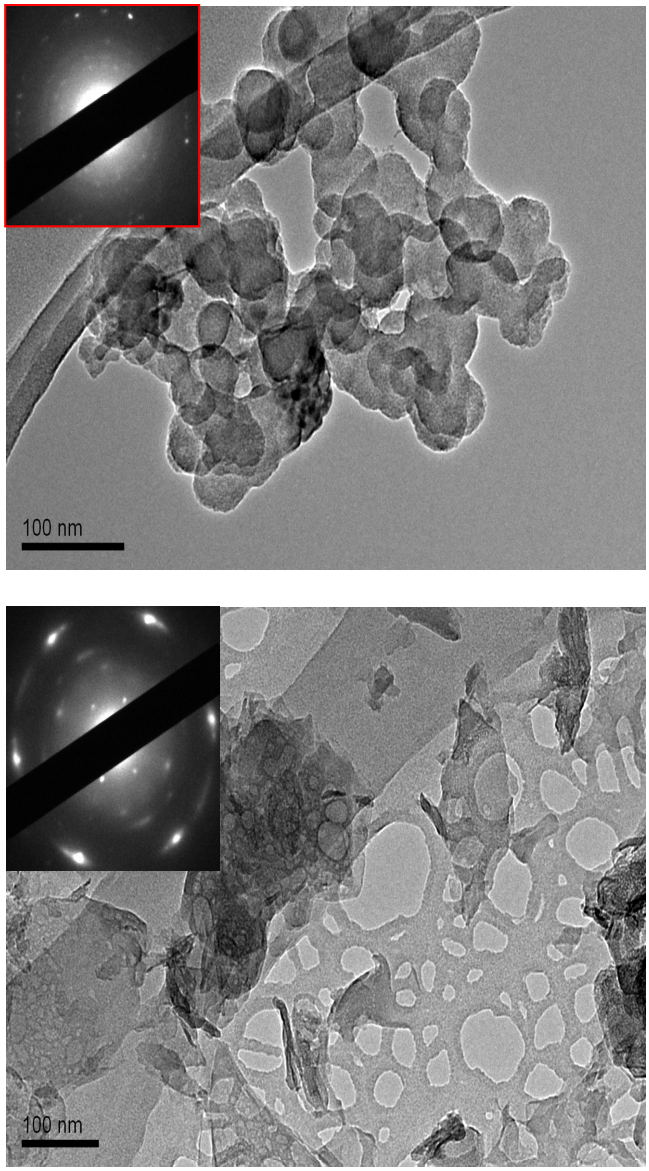

Figure 4. TEM morphology of Al−Li−X alloy before and after hydrolysis.

has bad hydrogen generation performance. However, the maximum percentage of nano particles in the milled mixture is small and the largest value is less then 4% in Fig. 5. Combined with Fig. 6 which shows SEM morgraph of milled Al-Li-X alloy. Due to the repeated cold welding and fracturing in the milling process, the particles are irregular, often agglomerated and their size distribution varies from 1 um to 52 um. The particle size was decreased with the addition of other metals (Bi, Sn, In, Ga) and smaller particles have larger specific surface area which tend to generate hydrogen quickly. The spatial elemental distribution in individual particles was analyzed by EDS mapping. Combined with XRD results in Fig, 2, LiX-dominant areas could be distinguished clearly in Al powder. The active center area (LiX− Al) was helpful to simulate aluminum hydrolysis in water.

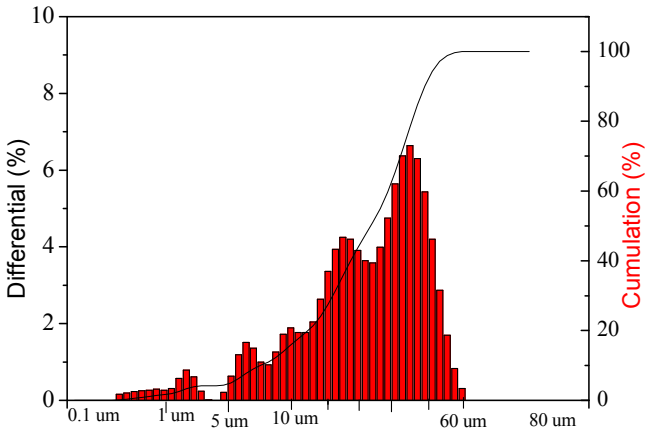

Figure 5. PSA analysis report of Al-Li-In alloy after hydrolysis.

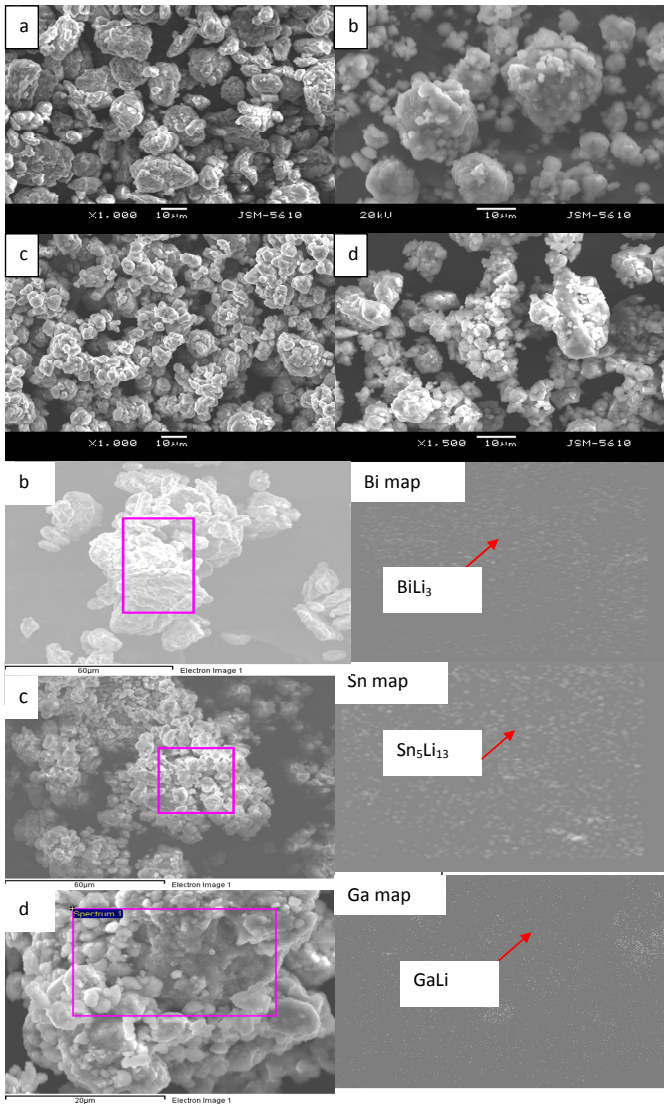

Figure 6. SEM images and metal map of Al-Li alloys. a, Al-10 wt.%Li; b, Al-10 wt.%Li-5 wt%Bi; c, Al-10 wt.%Li-5 wt%Sn; d, Al-10 wt.%Li-5 wt%Ga.

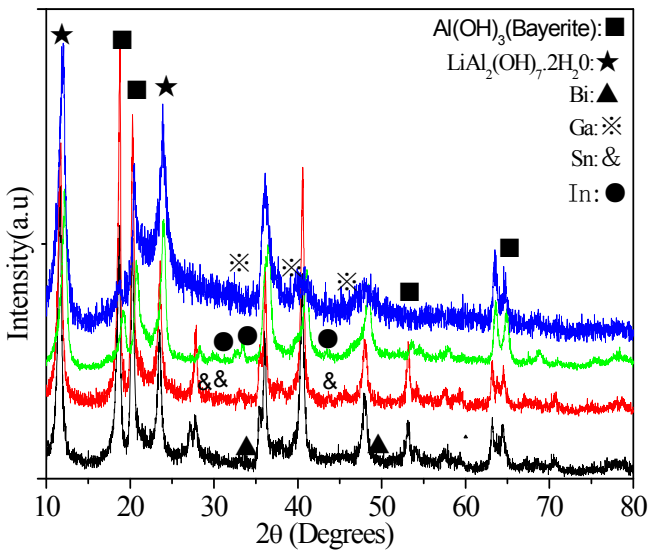

Figure 7. Shows XRD patterns of different milled Al-Li-X alloys after hydrolysis.

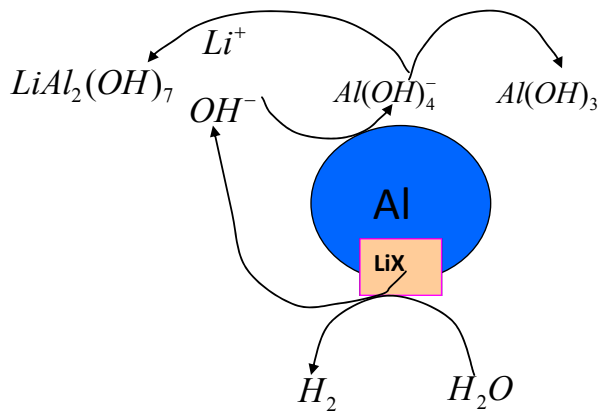

Figure 8. Schematic hydrolysis mechanism of Al-Li-X alloy in water

3.3. Hydrolyisis mechanism

Evidently, the improved hydrogen generation performance mostly came from lithium amount and other metal additives in the composite as the milled Al particles seldom react with water at 298 K. The fresh surface of the milled alloy supply large specific area for the connection of individual H_2O molecule and Al alloy. It has been explained that LiOH from Li hydrolysis stimulated Al hydrolysis in the chemical reactions (1-3). The hydrolysis byproducts can be identified from Fig. 7 which shows XRD patterns of different milled Al-Li-X alloys after hydrolysis.

$$2Li \quad + \quad 2H_2O \longrightarrow 2LiOH + H_2 \qquad (1)$$

However, there may exists different hydrolysis process of the Al-Li-X alloy in water with the other metal additives. Except the existence of $Al(OH)_3$ and $LiAl_2(OH)_7$, the peaks of metal additives are identified. The hydrolysis of Al alloys including Al-Bi, Al-Sn, etc., was based on the work of micro-galvantic fuel between Al (anode) and other metals (cathode) [11]. The other metal additives made the potential of aluminum shift negatively and reduced overpotential of hydrogen generation. The electrochemical corrosion of Al alloy could be elaborated in the reaction (4-6) and the connection of Al and X acted as the hydrolysis centers while the standard potentials of Al alloys listed in table 2 are lower than that of water decomposition.

But there are LiX and AlLi alloy except Al-X alloy in the Al-Li-X alloy. It is necessary to explore what reactions take place and which of them prevail in the whole corrosion reaction. LiX alloys have lower standard potentials than those of AlX alloys in Table 2. So the LiX alloys should replace AlX alloy and take as the initial hydrolysis centers when Al-Li-X alloys react with water. It is now possible to propose a general mechanism (depicted in Fig. 8), in order to describe the behavior of Al corrosion activated by Li and other metals X. In the micro galvantic cell of LiX, Li metal as a sacrifice anode combines with OH^- to generate LiOH and releases an electron in reaction 7. The H^+ is reduced to H atom on the surface of X metal in reaction 9 via obtaining an electron and two H atom are combined to H_2 molecule therefore.Then the hydrolysis byproduct LiOH further accelerated the hydrolysis of AlX alloys based on the micro-galvantic cell in reaction (8, 9). The hydrolysis of Al-Li-X alloy is based on the dual micro-galvantic fuels and a synergetic promoting mechanism is involved in the hydrolysis of Al-X alloy in the hydrolysis process [19]. The metal additives act as the cathode and stimulate the electrochemical corrosion of Li and Al. In addition, the by-product LiOH also stimulates the hydrolysis kinetic of reaction (2). There exists the competition between electrochemical corrosion and chemical reaction of Al which is determinated by the Li/X weight ratio. The LiX has quick hydrolysis kinetic and the highest quantity of Al connects with water, which results in the maximum hydrolysis rate occuring at the beginning of the reaction.

Table 2. Main phase and standard potential of LiX and AlX in the Al-Li-X alloy.

No.	Main phase composition	Standard Potential of LiX	Sandard Potentialof AlX alloy
Al-Li-Bi alloy	$BiLi_3$, AlLi, Al,	$BiLi_3$, −3.332 V	AlBi, -1.85 V
Al-Li-Sn alloy	Sn_5Li_{13},AlLi,Al,	Sn_5Li_{13}, -2.9 V	AlSn, -1.56 V
Al-Li-In alloy	$AlInLi_2$,AlLi, Al	$AlInLi_2$, -2.7 V	AlIn, -1.31 V
Al-Li-Ga alloy	GaLi,AlLi, Al	GaLi, -2.5 V	AlGa, -1.17 V
Al-Li alloy	AlLi, Al	Al, -1.67 V	no

After some time, the by-product $Al(OH)_3$ will combine with LiOH and produce $LiAl_2(OH)_7$ in reaction (3). The $LiAl_2(OH)_7$ and $Al(OH)_3$ concentration attain a critical value and accumulate on the Al particles, resulting in the mechanism change to one controlled by mass transfer in the product layer. The micro galvantic cell between Al and X could locally prevent the Al repassivation after hydrogen generation start [20].

In Fig. 6, it has been demonstrated that the uniform distribution of metal additives and Li in Al matrix is obtained, which favors to creating many active LiX-Al centers and forms micro galvantic cells in water. Therefore, the hydrogen generation performance can be improved via increasing X amount, increasing Li amount and uniform distribution of X in Al matrix. Increasing X amount and uniform distribution of X in Al matrix are helpful to creat more micro galvantic cells in water and improve the hydrogen generation performance of Al-Li-X alloys correspondingly. Increasing Li amount is explained that Li hydrolysis generates more hydrogen and its hydrolytic by-product LiOH and heat stimulates Al hydrolysis.

4. CONCLUSIONS

The milled Al-Li alloys in cluding low melting point metals such as Bi, Sn, In and Ga have good hydrogen generation performance at 298 K, especially that Al-10 wt.%Li-5 wt.% Bi alloy yields Al-10 wt.% Li-5 wt.%Bi alloy yields 1258 ml hydrogen/g with 95% efficiency and 594 ml /min.g maximum hydrogen generation rate. The presence of metal additives has a double effect. They reduce the grain size of Al-Li alloys due to the formation of new intermetallic compounds such as $BiLi_3$, Sn_5Li_{13}, $AlLiIn_2$, etc. The metal additives also strongly accelerates hydrogen generation rate as the metal additives on the Al and Li surface can act as cathodic centers with a lower over potential for hydrogen generation. It has been demonstrated that dual micro galvantic cells between Al (Li) and metal additives are generated in the hydrolysis process and stimulated the electrochemical corrosion of Al and Li correspondingly. The LiX acts as the initial hydrolysis centers due to its low standard potential and its hydrolysis byproduct LiOH further accelerates the micro galvantic cell between Al and X. Therefore, hydrogen generation performance is linked to standard potential of metal additives, increased Li and X amount, uniform distribution of Li and X in the Al matrix in the longer milling time. Our results show that the potential good hydrogen generation performance can be obtained via the design and preparation technology of Al alloys.

5. ACKNOWLEDGMENTS

This work was financially supported by the National Natural Science Foundation of China (Project No. 21003112 and 21003111), the Zhejiang Basic Research Program of China (No. Y4090507) and the Zhejiang Analysis Test Project of China (No. 2009F70010).

REFERENCES

[1] Lattin W.C., Utgikar V.P., Int. J. Hydrogen Energy, 32, 3230 (2007).
[2] Dincer I., Int. J. Hydrogen Energy, 27, 265 (2002).
[3] Neef H.J., Energy, 34, 327 (2009).
[4] Demirici U.B., Akdim O., Miele P., Int. J. Hydrogen Energy, 34, 2638 (2009).
[5] Franzoni F., Milani M., Montorsi L., Golovitchev V., Int. J. Hydrogen Energy, 35, 1548 (2010).
[6] Wang H.Z., Leung D.Y.C., Leung M.K., Ni M., Renewable and Sustainable Energy Review, 13, 845 (2009).
[7] Hunter M.S., Fowle P., J. Electrochem. Soc., 103, 482 (1956).
[8] Wang E.D., Shi P.F., Du C.Y., Wang X.R., J. Power Sources, 181, 144 (2008).
[9] Deng Z.Y., Liu Y.F., Tanaka Y., J. Am. Ceram. Soc., 88, 977 (2005).
[10]Czech E., Troczynski T., Int. J. Hydrogen Energy, 35, 1029 (2010).
[11]Fan M.Q., Sun L.X., Xu F., Int. J. Hydrogen Energy, 32, 2809 (2007).
[12]Kravchenko O.V., Semenenko K.N., Bulychev B.M., Kalmykov K.B., J. Alloys Comp., 397, 58 (2005).
[13]Nagira K., Shimizu T., Method of producing hydrogen and material used therefor., US patent 1988; 475, 2463.
[14]Ilyukhina A.V., Kravchenko O.V., Bulychev B.M., Shkolnikov E.I., Int. J. of Hydrogen Energy, 35, 1905 (2010).
[15]Fan M.Q., Sun L.X., Xu F., Energy, 35, 2922 (xxxx).
[16]Grosjean M.H., Zidoune, Huot J.Y., Int. J. Hydrogen Energy, 31, 1159 (2006).
[17]Seith W., Kubaschewski O., Elektrochem., 43, 743 (1937).
[18]Su Y.C., Yan J., Lu P.T., Solid State Ionics, 177, 507 (2006).
[19]Soler L., Candela A.M., Macanas J., Munoz M., Casado J., Int. J. Hydrogen Energy, 35, 1038 (2010).
[20]Nestoridi M., Pletcher D., Wood R.J.L., Wang S., Jones R.L., J. Power Sources, 178, 445 (2008).